Effects of hydrodynamic instability, plate size and geometry on heat flux in pool boiling

Elena Agostoni[1]

[1] Department of Energy Engineering, Politecnico di Milano, Via Lambruschini 4 Milano, Italy
Corresponding author e-mail: elena.agostoni@mail.polimi.it

Abstract. In the last century, as the need for pool boiling for industrial and energy applications increased, so did the need for reliable models predicting heat flux behaviour. Zuber's pioneering approach, based on the effects of hydrodynamic instability, was the first to give the scientific community predictive correlations for the minimum and maximum or critical heat flux in pool boiling. Years later Lienhard refined the model, adding factors for different shapes and sizes of plates. To conclude, a comparison between the two models is given, demonstrating the improvement gave by Lienhard on the already solid base of Zuber's model.

1. Introduction

The last century saw the development of nuclear physics and engineering, and with it came the building of the first nuclear reactors and nuclear power plants. Their components work in particular operating conditions (e.g. high pressure and temperatures), and thus the designers needed to base their projects on reliable models and correlations describing the physical phenomena happening in the systems.

A particular feature of nuclear reactors is the presence of high heat transfer rates across small areas, which is given by a pool boiling process. Forced convection boiling at such high heat transfer rates would need very high flow speeds and cause a subsequently high pressure drop.

Unfortunately, the scientists and researchers (from the 1940s onward) soon discovered that a complete and reliable description of pool boiling offered many challenges. One of the difficulties came from the fact that the data available to validate the correlations was still poor because of the many technological limitations existing back then. Even after the engineers were able to overcome some technical limitations, it was evident that the phenomena were complex also from the physical point of view. Notably, relevant parameters are bubble dynamics and interaction, together with surface roughness, pipe geometry, inclination and size, rheological properties of the fluids, and many more. First approaches to try and describe pool boiling considered most of these effects as separate contributions, but they are instead deeply interconnected, so no general relation could be inferred.

The pessimism that spread in the scientific community around obtaining a reliable and general correlation for pool boiling has found a new hope, thanks to the new micro-fabricated surfaces and powerful numerical codes available nowadays [1].

2. General description of pool boiling

Pool boiling is composed of 3 different boiling modes, as can be seen in Figure 1: nucleate boiling (NB), transition boiling (TB) and film boiling (FB). Each one of them is characterized by processes that are unique to that given mode, and between them liquid-gas distribution and interaction changes

drastically, subsequently also changing the heat transfer performance (ruled by the heat transfer coefficient α)

$$\alpha_{NB} > \alpha_{TB} > \alpha_{FB} \tag{1}$$

Nuclear reactors systems will not operate in all of the modes of pool boiling. Nucleate boiling is the smartest choice of operating conditions, given for example the fact that it has the best heat transfer performance and mode stability [2].

Going back to describing the boiling modes, the lower bound of NB is natural convection of a one-phase liquid. This liquid will be saturated to a surface superheating $\Delta T_{S,Sat}$, necessary for the superheating of a thin film of liquid over the surface. This will lead to the onset of nucleate boiling. Increasing $\Delta T_{S,Sat}$, the bubble population will increase sharply, up to a point where bubbles interact and merge. The motion of bubbles acts as mixing, aiding in the heat transfer process.

The heat flux to the surface $q_s^{''}$ will reach its maximum at the upper bound for NB: the condition of critical heat flux (CHF). Around this point, hydrodynamic instabilities play a major role in the process. At TB the merging bubbles locally coat the surface with a layer of thermally insulating vapor film, impeding contact between the liquid and the surface. This will worsen the heat transfer and in TB $q_s^{''}$ will decrease down to a minimum value.

A global vapor film will coat the surface at even higher $\Delta T_{S,Sat}$, in the region of film boiling. In this paper FB will not be analyzed, since operating in this region can quickly lead to meltdown of the component.

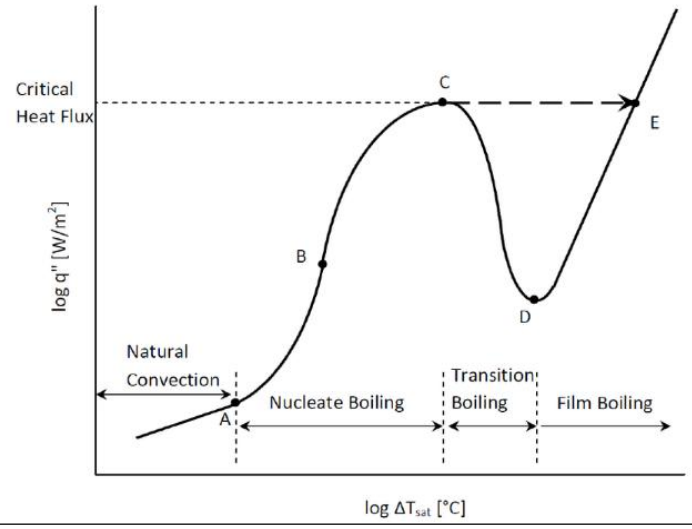

Figure 1. Nukiyama's pool boiling curve, showing the functional dependence of the heat flux and surface superheating. AC represents nucleate boiling, being AB the region for isolated bubble generation and BC the region with bubble columns and jets. C is the critical heat flux region. CD represents transition boiling and DE film boiling.

For nuclear design purposes we are involved with systems that work at $q_s^{''} = \text{const}$, and the most vital feature is the estimation of CHF, acting as an upper bound for the operating conditions.

2.1. Understanding nucleate boiling

Heterogeneous boiling is a phenomenon which starts from the heated surface, and it begins at the wall's imperfections, where we find nucleation sites given by imperfect wetting of the cavities. Given a cavity that we can suppose to be of conical geometry for the sake of simplicity, the radius at which a bubble detaches must be greater than a critical radius. This means that the superheating needed for bubble detachment must be greater than the superheating needed to reach the critical radius.

Most of the functional dependencies $q_s^{''} = \text{function}(\Delta T_{S,Sat})$ are described by power laws

$$q_s^{''} = \text{constant}\,(T_s - T_{sat})^n \tag{2}$$

where the exponent in most correlations in the nucleate boiling region is around 3, as we can see in both the Cooper's and Rosenhow's models [1]. The constant that appears in equation (2) also depends on the surface characteristics (from its polishing, for example). Thus, a time dependence should theoretically be included since, over time, boiling changes the characteristics of the surface. We will discard such dependence by hypothesizing that after a long enough time exposed to boiling, all surfaces will appear similar.

Another assumption, that for now we will assume to be true, is the one Zuber made in his paper [3]: in NB the heat transfer rate is not affected by the geometry of the system, given the fact that bubbles induce strong localized agitation. The meaning of this assumption is that we can utilize the radius of the bubble as the characteristic dimension of our apparatus.

This assumption was also adopted years earlier by Rosenhow [4], which proposed a model that predicted the heat transfer coefficient of NB using dimensionless parameters: the Stanton (St), Reynolds (Re) and Prandtl (Pr) numbers. He linked them by an empirical relationship through a constant $C_{s,f}$ that depends on surface and fluid properties

$$\frac{1}{St} = C_{s,f}\,Re^{m}Pr^{n} \tag{3}$$

where m, n are determined experimentally. A model like Rosenhow's appears simple and has a good fit with the data, but since it is based on the behavior of a single bubble, it cannot predict the transition in boiling modes that happens at CHF. In fact, as Zuber pointed out [3], "maximum nucleate heat flux is brought about because of the mutual interference of many bubbles". In the next section we will study in greater detail the meaning behind such "interference".

2.2. Kutateladze's model

Over the years, many trigger mechanisms have been proposed for CHF. They are, as listed in Liang's work [5], bubble interference, microlayer dry out, hot/dry spots, interfacial lift-off, and hydrodynamic instability. The latter phenomenon is the one we are interested in, and its contribution to CHF can be understood by analyzing first of all the work by Kutateladze [6].

According to him, CHF is achieved when critical velocity of the vapor phase is reached. He also made the hypothesis that all the heat flux provided to the surface was used to evaporate the liquid. Thanks to dimensional analysis and a balance of inertia, buoyancy and surface tension forces for a bubble, he experimentally derived the constant K, also called Kutateladze's constant

$$K = \frac{q_s''}{\rho_g h_{fg}\left(\frac{\Delta\rho\, g\, \sigma}{\rho_g^2}\right)} \sim 0{,}16 \tag{4}$$

where ρ_f is the liquid's density, ρ_g is the one of the gas and $\Delta\rho = \rho_f - \rho_g$ the difference between the two. σ is the superficial tension and g the gravitational acceleration, h_{fg} is the latent heat of evaporation.

A mechanistic prediction of K came years later with the Zuber's model for CHF, based on Kutateladze's work.

2.3. Critical heat flux and Transition boiling

While approaching critical heat flux, there is a steady movement of liquid towards the surface and of vapor away from it [6]. A larger part of the surface's area will be occupied by vapor rather than liquid, and bubble columns or jets of vapor will surround filaments of liquid that will reach the surface, only to evaporate and feed again the jet mechanism. The shape and geometry of the jets and filaments is still random (unlike what is seen in transitional boiling, see below in this section), and one could say that while in NB we have liquid surrounding vapor (with isolated bubbling), here we start to have vapor surrounding liquid filaments. Transitional boiling is reached when the vapor jets reach a critical

velocity, making it impossible for the filaments to reach the surface. We can thus say that in NB we had liquid-surface contact, while in the TB region the Leidenfrost phenomenon [7] starts to occur locally, meaning that the liquid will take the shape of a spheroid and will "hover" over a thin layer of vapor. This will impede local liquid-surface contact in TB. Later studies [8] demonstrated the presence of liquid-surface contact, although it may be negligible.

Another characteristic of TB that was not present in NB is the well-defined geometry of the flow: the random motion of bubbles in NB is substituted by a release at regular intervals of bubble columns. These facts suggest that a new mechanism which we did not see in NB is instead present in TB: the hydrodynamic instability, or more precisely, Taylor Rayleigh (TR) instability and Kelvin Helmholtz (KH) instability.

A surprising advancement was brought forward by Perkins and Westwater [9]: CHF is spread over a range of temperatures where heat flux is stable. This indicates the coexistence of NB and TB. It also suggests that while we have hydrodynamic instability, we have thermal stability.

3. Hydrodynamic instability

3.1. Taylor Rayleigh instability

Taylor Rayleigh (TR) instability [10] is a hydrodynamic phenomenon happening when we have two fluids of different densities, for example vapor and liquid, in contact with one another. The denser liquid lays on top of the less dense vapor, making the interface that separates them unstable. The two fluids are accelerated perpendicularly to the interface, and this will cause irregularities in the interface itself which, given its instability, will grow in amplitude in time in an exponential way.

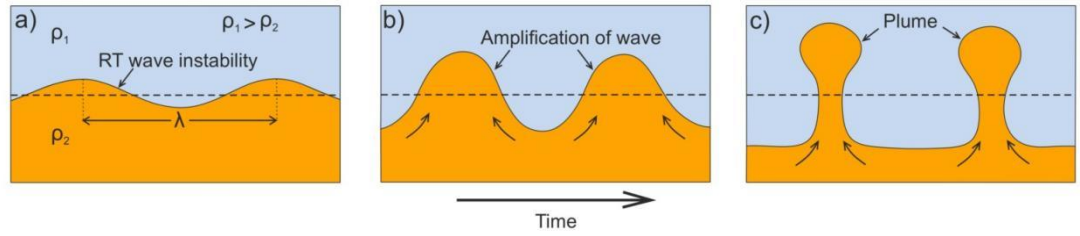

Figure 2. Time evolution of TR instability. ρ_1 is the liquid's density, and ρ_2 is the vapor density.

One could imagine that these disturbances spread throughout the surface with a sinusoidal function with certain wavelength λ_t, called Taylor wavelength. The condition of instability is granted by the fact that λ_t is between the values of a critical wavelength λ_c and a "most dangerous" one λ_d, which represents the fastest spreading wavelength of instability.

$$\lambda_c \leq \lambda_t \leq \lambda_d \tag{5}$$

$$\lambda_c = 2\pi \left[\frac{\sigma}{g(\rho_f - \rho_g)}\right] = 2\pi L_c \tag{6}$$

$$\lambda_d = \sqrt{3}\,\lambda_c \tag{7}$$

L_c is called Laplace length and it describes the bubble's characteristic length, the radius. During the final stages of NB, as nucleation rate rises, a region of the heater's surface is locally coated with vapor that accelerates towards the liquid, a denser fluid. If the acceleration is such that equation (5) is verified, we will have TR instability.

The geometric regularity of the process can be deduced not only from the sinusoidal and regular function describing it, but also from the fact that the phenomenon arises away from the surface. We have already seen how in NB the nucleation process is strictly linked with the surface and its random

defects, cavities and local differences. With TR instability such random elements are taken out of the equation, leaving just parameters defined by the fluid's properties. The regularity of the geometry also implies a regularity in the discharge of bubble columns or jets, depending on the intensity of the heat flux.

With TR, that fact that a variation in heat flux coincides with changes of the instability's wavelength (or frequency), will mean that $q''_{s,max}$ corresponds to the maximum frequency, and $q''_{s,min}$ corresponds to the minimum frequency.

3.2. Kelvin Helmholtz instability

Around CHF there is the presence of another hydrodynamic instability: the Kelvin Helmholtz instability (KH) arising when, at a critical velocity, there is relative motion parallel to the interface between two fluids. We can see the phenomenon very clearly in Figure 3a and Figure 3b. Because of the velocity difference between vapor and liquid, the surface of the vapor jets incurs in Helmholtz instability, which will grow and cause merging of adjacent jets [6]. Indeed, velocity must be considered in the model and in particular we must find the critical velocity at which KH instability happens.

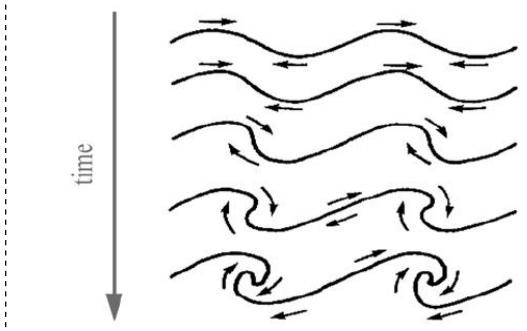

Figure 3a. Helmholtz instability evolution over time.

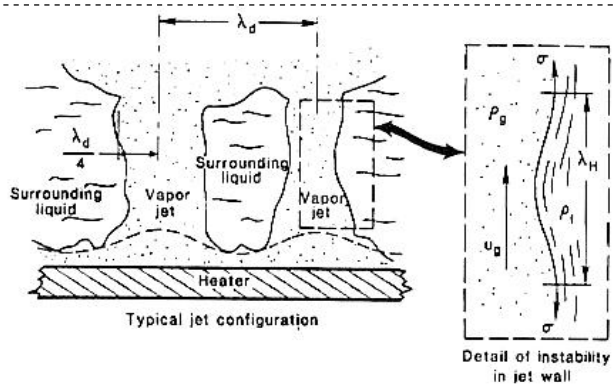

Figure 3b. Hydrodynamic instability in action.

Before going forward with the derivation of the model, it is important to underline that Zuber [3] determined that $q''_{s,max}$ is characterized by the combined effects of TR and KH, while $q''_{s,min}$ is characterized just by TR instability.

4. Deriving Zuber's model for an infinite flat surface

Let us now derive the Zuber [3] model, based on Kutatekadze's work [6]. Its aim is not only to correlate existing data, but also to predict the minimum and maximum heat flux. Even if the global takeaway of the theory is valid, some misapprehensions were involved in Zuber's description, as was pointed out by Lienhard [8], but we will outline them later in the paper.

Let's take a jet of diameter D_j and hypothesize that it will have the characteristic length of a bubble, L_c. The limits for such length will be given by equation (5), (6) and (7) via simple substitution.

$$D_j = \frac{\lambda_t}{2} \tag{8}$$

Zuber assumed that the surface of TR instability could be modeled by repeating square cells, as we can see in Figure 4, each one containing a vapor jet on every vertex, a center jet and liquid surrounding them. Thus, each cell will have length equal to λ_t.

Be it A_g the area occupied by the jet and A_w the area occupied by the heater, it is trivial to demonstrate that

$$\frac{A_g}{A_w} = \frac{\pi}{16} \tag{9}$$

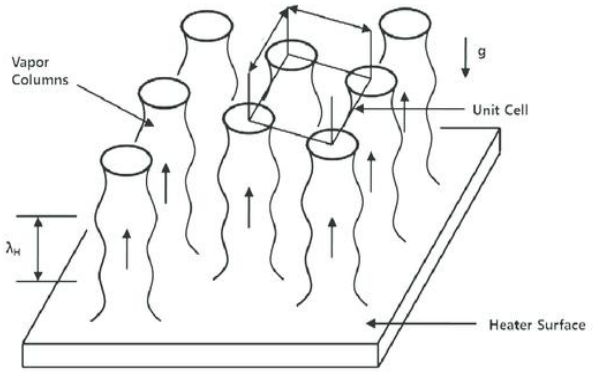

Figure 4. The unit cell that Zuber used in his model.

Let us call the velocity of the jets emanating from the surface u_g and u_f the velocity of the liquid filaments reaching towards the surface. Just before CHF we can impose continuity between the velocity of the phases and obtain

$$u_f = \frac{\rho_g A_g u_g}{\rho_f (A_w - A_g)} = \frac{\rho_g}{\rho_f}\left(\frac{A_g / A_w}{1 - A_g / A_w}\right) u_g = \tag{10}$$
$$= \frac{\rho_g}{\rho_f}\left(\frac{\pi}{16 - \pi}\right) u_g$$

As both Zuber and Kutateladze assumed, all the heat flux arriving to the surface will be used for evaporation.

$$q''_{s,max} = \frac{\rho_g A_g u_g h_{fg}}{A_w} \tag{11}$$

$$u_g = \frac{q''_{s,max}}{\left(\frac{\pi}{16}\right)\rho_g h_{fg}} \tag{12}$$

4.1. Prediction of maximum heat flux

For Zuber, the critical heat flux is reached when the jets become Helmholtz unstable. The jets will serve as the escape route for vapor, until the vapor's velocity is high enough to make the jets Helmholtz unstable. This defines $q''_{s,max}$ in NB, or CHF.

The Helmholtz instability is given by a difference in phase velocity, which can be expressed as

$$u_g - (u_f) = \left(\frac{\rho_g + \rho_f}{\rho_f}\right)^{1/2} \left(\frac{\sigma}{\rho_g \mathrm{L_c}}\right)^{1/2} \tag{13}$$

$$\lambda_H = \pi \, \mathrm{D}_j = 2\pi \, \mathrm{L_c} \tag{14}$$

λ_H is the critical Helmholtz wavelength, the one that is amplified and becomes unstable. Zuber hypothesized λ_H to be equal to the Rayleigh wavelength, meaning a wavelength equal to the circumference of the jet.

The instability arises if equation (13) is not zero. If we suppose that $\rho_f \gg \rho_g$, the critical velocity U, based on Helmholtz's wavelength, is

$$U = \left(\frac{2\pi\sigma}{\rho_g \lambda_H}\right)^{1/2} \tag{15}$$

substituting the needed equations, Zuber finally obtained $q''_{s,\,max}$

$$q''_{s,\,max} = C\frac{\pi}{24}\rho_g h_{fg}\left[\sigma g\left(\rho_f - \rho_g\right)\right] \tag{16}$$

where C is a constant depending on the choice of wavelength (e.g. critical or most dangerous), with a value that can be approximated to C=1. This expression led Zuber to find the value of K, equation (4), in a mechanistic way.

4.2. Prediction of minimum heat flux

In TB there is presence of a vapor blanket. We can allow contact between liquid and surface only if the blanket's interface collapses on the surface. $q''_{s,\,min}$ is reached when the heat flux matches the latent heat removal that sustains TR instability waves, meaning that any heat flux lower than that will not produce vapor fast enough to lift the interface. Thus, the interface will collapse onto the plate, cooling it by re-establishing liquid-surface contact, and we will return to NB.

Zuber considered the rate of collapse, and his prediction took the form of

$$q''_{s,\,min} = (Q_{LH})(N_b)(\nu_{min})(N_A) \tag{17}$$

given a bubble of diameter $\lambda_d/2$, the latent heat transfer Q_{LH} per bubble will be

$$Q_{LH} = \rho_g h_{fg}\left(\frac{2\pi}{3}\right)\left(\frac{\lambda_d}{4}\right)^3 \tag{18}$$

N_b is the number of bubbles per wave oscillation and it will be equal to 2 (1 bubble per half circle). N_A is the number of bubbles per surface area, and it corresponds to $1/\lambda_d^2$. ν_{min} is the minimum number of oscillations per unit time. The derivation of such value is quite tedious, so we will just analyze the functional dependence

$$\nu_{min} \sim \left[\frac{g\left(\rho_f - \rho_g\right)}{\rho_f \lambda_\mathrm{d}}\right] \tag{19}$$

Substituting in equation (17), we finally obtain

$$q''_{s,\,min} = C\rho_g h_{fg}\left[\sigma g \frac{\rho_f - \rho_g}{\left(\rho_f - \rho_g\right)^2}\right]^{1/4} \tag{20}$$

where now C=$(\pi^2/60)(4/3)^{1/4}$.

4.3. Discussing the results

Zuber's work was a pioneering piece and still offers a valid model to base ourselves onto. But it is far from perfect.

The data he used were few and most of the time of bad quality (especially true for determining $q''_{s,\,min}$). Lienhard [8] outlines some of the problem with Zuber's formulation, and among what he reported, we will focus on some of the most evident issues:

1. Unlike Zuber hypotesized, there is surface-liquid contact in TB, even if it might be negligible.
2. A more correct analysis of hydrodynamic instability should be 2-dimensional.
3. He assumed that there is no contribution from the system's geometry.
4. He set bubbles and jets with the same radius, which seems too arbitrary.
5. The choice of the most dangerous wavelength over the critical wavelength (or vice versa) is unclear most of the time.

Furthermore, Zuber formulated the model for an infinite and flat heater plate: an optimal assumption for the simplification of the derivation (e.g. no boundary conditions needed), but a case that is far from reality.

Our next step is to try to assess what happens with plates with different sizes and geometries, to check how they would affect Zuber's model.

5. Expanding the model to plates with different size and geometry

In 1973 Lienhard published a paper [8] whose aim, between many others, was to extend Zuber's theory [3] to plates with geometries and sizes different than the flat and infinite plate Zuber analyzed in his model. In fact, many assumptions Zuber made need to be investigated further. Starting from λ_H: Zuber's choice of the Rayleigh wavelength is valid as long as the heater, and therefore the jet, are small. Larger bodies will in fact induce larger jets and the Rayleigh wave will become larger than λ_d. This means that the jets might collapse at a lower vapor velocity than the critical Helmlotz's velocity, as we can see in equation (15).

Lienhard showed that Zuber's model gave values about 14% smaller than what is experimentally found for a infinite flat plate, $q''_{s,\,max,Flat,\,Infinite}$.

$$\frac{q''_{s,\,\mathrm{max,Flat,\,Infinite}}}{q''_{s,\,\mathrm{max,\,Zuber}}} = 1.14 \tag{21}$$

From now on we will refer to "infinite plates" as plates whose dimensions vastly exceed the value of λ_d. Furthermore, the plates must be surrounded by vertical walls to avoid the disturbance of surrounding liquid. Experimentally, an infinite plate must not only respect the formerly mentioned criteria, but it also should be "clean". Unfortunately, many of the data Lienhard encountered came from "dirty" heaters, or from fluids with low purity or coming from unknown mixtures, and needed to be discarded.

5.1. Expanding the model

We have considered the validity conditions of Zuber's assumption, and should now note that such constraints exist because as soon as the plate's dimensions approach λ_d, A_g/A_w starts to vary discontinuously. Let us follow Lienhard's [11] analysis and see how.

A very small plate may accommodate just one single jet, but as we increase the size of the plate, more and more jets will need to be accommodated, all needing not to lie any closer than $\lambda_\mathrm{d}/4$ from

the plate's walls. Thus, as we increase the number of jets, the geometry of disposition varies to follow the constraint given by the distance from the wall. Following this condition, the heat flux for a plate will be

$$q_s'' = q_{s,\text{Infinite}}'' \left(\frac{N_j \lambda_d^2}{A_w} \right) \tag{22}$$

where N_j is the number of jets on a plate. This reasoning can be applied not only to plates with different sizes but also different shapes.

Lienhard [11] produced an extensive overview of different geometries like small/large cylinders, small/large spheres etc. In fact, he underlined that the geometry of a finite body influences both the size and placement of the jets (e.g. a small cylinder will have small jets). Figure 6 succeeds at giving a graphic representation of some of the geometries evaluated by Lienhard.

He confronted experimentally his predictions but, as we said before, he also faced the problem of not being able to produce or find enough adequate data. For example, for a circular finite plate he found just one valid data point. We will thus not focus on the discussion of those experimental results, and just evaluate how they relate to Zuber's predictions.

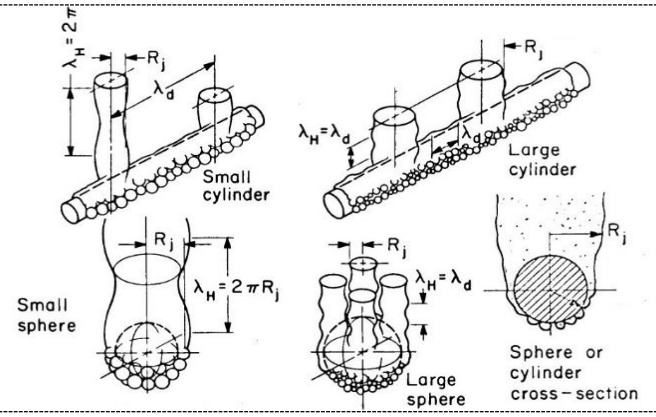

Figure 6. Different heater geometries (cylinder and sphere) and sizes (small and large), and different jets they create. Note that $R_j = D_j/2$.

5.2. Discussing the results

$$\frac{q_{max}''}{q_{max,Zuber}''} = \frac{24}{\pi} \frac{A_g}{A_w} \left(\frac{2\pi}{\lambda_d \sqrt{g(\rho_f - \rho_g)/\sigma}} \right)^{1/2} \tag{23}$$

In the case of infinite heaters, we will once again obtain equation (21). In Table 1 we will instead offer some of the results found by Lienhard [11].

Table 1. Results for different geometry and sizes.

	$\frac{A_g}{A_w}$	$\frac{q_{max}''}{q_{max,Zuber}''}$
Large cylinder	0.155	0.904
Large spheres	0.143	0.84
Generic large heater	0.155	0.9
Small cylinder	0.171	$0.904/\sqrt[4]{R'}$
Small spheres	0.220	$1.754/\sqrt{R'}$
Infinite flat plate	0.19	1.14

R' is the Rayleigh number and represents the ratio between buoyant and capillary forces. When R'=1, we no longer have capillary force.

A collective prediction for all large heaters could be made since it is evident from Table 1 that the ratio of the areas is almost constant. The same cannot be said for a generic small body, where an analysis case-by-case is required.

Finally, we can conclude that, especially for large heaters, Lienhard's model varies of just about 22%-27% from Zubert's predictions, even if his model was under very simplified assumptions.

6. Conclusions

In this paper, Zuber's model is presented as a solid base for the understanding of the hydrodynamic instability mechanism and how it affects boiling modes. Furthermore, Zuber also satisfied the need in engineering and design to have accurate and reliable correlations to determine critical heat flux.

Some of the assumptions Zuber made needed to be investigated more in depth. In this work we have focused in particular on correcting the infinite flat plate geometry that was the base for Zuber's correlation, and to do that we relied on Lienhard's work. It was subsequently made evident how placement and size of the jets was influenced by the surface geometry and size, and this led us to find different values of A_g/A_w.

Using those newly found values, we were finally able to obtain how much the correction of the q''_{max} predicted by Zuber would amount to. It was found that the correction by Lienhard for large heaters in different geometries varies of roughly 25% from the one by Zubert.

It is to be noted that many years have passed since the publishing of both Zuber′s paper (1958) and Lienhard′s paper (1973). The lack of experimental data that the two scientists had to face due to technological difficulties obviously affected the quality of the correlations. Thus, an interesting future development and expansion of this paper would be to experimentally test the corrected Zuber′s correlation on micro-fabricated surfaces and/or with numerical codes. This would aid in refining the experimental conditions, and help us broaden the dataset with useful data.

References

[1] Dhir V K 2006 Mechanistic prediction of nucleate boiling heat transfer-Achievable or a hopeless task? *J. Heat Transfer*
[2] Adiutori E F New theory of thermal stability in boiling systems *Nucleonics*
[3] Zuber N, Tribus M 1958 Further remarks on the stability of boiling heat transfer (California Univ., Los Angeles Dept. of Engineering)
[4] Rosenhow W M 1952 A method of correlating heat transfer data for surface boiling of liquids (Trans. ASME)
[5] Liang G, Mudawar I 2017 Pool boiling critical heat flux-Part 1 *J. Heat Transfer*
[6] Kutateladze S S 1948 On the transition to film boiling under free convection *Kotloturbostoenie*
[7] Drew T B, Mueller A C 1937 Boiling (Trans.)
[8] Lienhard J H, Witte L C 1985 An historical review of the hydrodynamic theory of boiling *Reviews of chemical engineering*
[9] Perkins A S, Westwater J W 1956 Measurements of bubbles formed in boiling methanol *AIChE Journal*
[10] Taylor G I 1950 The instability of liquid surfaces when accelerated in a direction perpendicular to their plane (London, Proc.)
[11] Lienhard J H, Dhir V K 1973 Extended hydrodynamic theory of the peak and minimum pool boiling heat fluxes (Kentuky Univ., Lexington)